JBC Papers in Press. Published on April 14, 2014 as Manuscript M113.543504
The latest version is at http://www.jbc.org/cgi/doi/10.1074/jbc.M113.543504

Atypical OmpR/PhoB Subfamily Response Regulator GlnR of Actinomycetes Functions as a Homodimer, Stabilized by the Unphosphorylated Conserved Asp-focused Charge Interactions

Wei Lin(林炜)[1], Ying Wang（王颖）[1,3], Xiaobiao Han（韩小彪）[1], Zilong Zhang（张子龙）[1], Chengyuan Wang（王程远）[2], Jin Wang（王金）[1], Huaiyu Yang (阳怀宇) [6], Yinhua Lu（芦银华）[1], Weihong Jiang（姜卫红）[1], Guo-Ping Zhao（赵国屏）[1,3,4,5*], Peng Zhang（张鹏）[1,2*]

[1]CAS Key Laboratory of Synthetic Biology, [2]State Key Laboratory of Plant Molecular Genetics, Institute of Plant Physiology and Ecology, Shanghai Institutes for Biological Sciences, Chinese Academy of Sciences, Shanghai 200032, China; [3]State Key Laboratory of Genetic Engineering, Department of Microbiology and Microbial Engineering, School of Life Sciences, Fudan University, Shanghai 200433, China; [4]Shanghai-MOST Key Laboratory of Disease and Health Genomics, Chinese National Human Genome Center at Shanghai, Shanghai 201203, China; [5]Department of Microbiology and Li Ka Shing Institute of Health Sciences, The Chinese University of Hong Kong, Prince of Wales Hospital, Shatin, New Territories, Hong Kong SAR, China; [6]Institute of Materia Medica, Chinese Academy of Sciences, Shanghai 201203, China

Running title: Structure and function of the receiver domain of GlnR

[*] Correspondence should be addressed to: G.-P. Zhao at gpzhao@sibs.ac.cn and P. Zhang at pengzhang01@sibs.ac.cn

Keywords: actinomycete, OmpR/PhoB subfamily GlnR, crystal structure, unphosphorylated aspartate, receiver domain, homodimer

Background: Orphan response transcription factor GlnR regulates nitrogen metabolism in important actinomycetes.

Results: GlnR has no typical "phosphorylation pocket", where the only conserved Asp is unphosphorylated but is essential for functional homodimerization.

Conclusion: Actinomycete GlnR is an atypical response regulator functioning as a homodimer.

Significance: Conserved Asp-focused charge interactions of actinomycete GlnR are likely the mechanism that stabilizes the homodimer for physiological function.

Summary

The OmpR/PhoB subfamily protein GlnR of actinomycetes is an orphan response regulator (RR) that globally coordinates the expression of genes related to nitrogen metabolism. Biochemical and genetic analyses reveal that the functional GlnR from *Amycolatopsis mediterranei* is unphosphorylated at the potential phosphorylation Asp50 residue in the N-terminal receiver domain. The crystal structure of this receiver domain demonstrates that it forms a homodimer through the α4-β5-α5 dimer interface highly similar to the phosphorylated typical RR while the so-called "phosphorylation pocket" is not conserved with its space being occupied by an Arg52 from the β3-α3 loop. Both *in vitro* and *in vivo* experiments confirm that GlnR forms functional homodimer *via* its receiver domain and suggest that the charge interactions of Asp50 with the highly conserved Arg52 and Thr9 in the receiver domain may be crucial in maintaining the proper conformation for homodimerization as also supported by molecular dynamics simulations of the wild type GlnR *versus* the deficient mutant GlnR(D50A). This model is backed by the distinct phenotypes of the total deficient GlnR(R52A/T9A) double mutant *versus* the single mutants of GlnR, *i.e.* D50N, D50E, R52A and T9A, which have only minor effects upon both dimerization and physiological function of GlnR *in vivo* albeit their DNA binding ability is weakened comparing to that of the wild type. By integrating the supportive data of GlnRs from the model *Streptomyces coelicolor* and the pathogenic *Mycobacterium tuberculosis*, we conclude that the actinomycete GlnR is atypical with respect to its unphosphorylated conserved Asp residue being involved in the critical R/D/T charge interactions, which is essential for maintaining the biologically active homodimer conformation. (260words)

Introduction

Two-component system (TCS), typically consisting of a membrane-associated sensor histidine kinase (HK) and a cognate intracellular response regulator (RR), is the predominant signal transduction system employed by bacteria, and also found in archaea and eukarya (1). Most typical RRs remain as monomers or "weak" dimers (2,3) with their receiver domains unphosphorylated. Once the environmental stimulus triggers HK autophosphorylation, the phosphoryl group is transferred to a conserved Asp residue in the receiver domain of the cognate RR. The phosphorylated RR then undergoes a substantial conformational change for "tight" homodimerization that enables its binding to the target DNA sequences (*cis*-elements) and in turn affects the transcription (4-6). Based on the homology of their DNA-binding domains, most RRs can be categorized into four major subfamilies, *i.e.*, OmpR/PhoB, NarL/FixJ , NtrC and LytR, leaving the remaining RRs containing miscellaneous effector domains such as RNA binding or enzymatic functions (2,7).

In most bacteria, a TCS is employed to sense and respond to the nitrogen status in the environment and the NtrB/NtrC-mediated nitrogen assimilation regulation in enteric bacteria is one of the best studied (8,9). However, in many actinomycetes, including the rifamycin-producing industrial actinomycete *Amycolatopsis mediterranei,* the model organism *Streptomyces coelicolor*, and the pathogenic *Mycobacterium tuberculosis*, nitrogen assimilation is globally regulated by an OmpR/PhoB subfamily protein, GlnR (10-13), which is considered an orphan RR because its cognate sensor HK has not been identified (10,11,14-16). Despite its great

importance in global regulation of nitrogen metabolism, the understanding of the regulation of GlnR activity as well as its impact upon the GlnR-mediated global transcription regulation is limited although much attention has been paid to the identification of the GlnR target genes and their corresponding *cis*-elements so far (10,13,17-19) .

The GlnR from *S. coelicolor* (ScoGlnR) was once predicted to be a typical RR subject to Asp phosphorylation as typical OmpR/PhoB subfamily members due to the presence of the conserved residues Asp50 and Thr83 of the active site quintet (14,20,21), essential in defining the so-called acidic "phosphorylation pocket" of the typical RRs (22). Recently, the atypical receiver domains of several orphan RRs (7,22,23) were shown generally similar to the typical receiver domains in their amino acid sequences and three-dimensional structures but lacked one or more residues of the highly conserved active site quintet (22,24). Because the GlnR from actinomycetes other than streptomycetes (ref to **Figure 2**) only has its putative phosphorylation site Asp residue found to be conserved in the active quintet (21,25), we hypothesized that GlnR is an atypical RR with its activity being independent of Asp phosphorylation. However, this hypothesis was mechanistically challenged by a mutational analysis, in which, substitution of the potential phosphorylation site Asp residue with Ala abolished the GlnR function in *Mycobacterium smegmatis* (14).

In this study, the structure-function relationship of GlnR from *A. mediterranei* (AmeGlnR) is comprehensively analyzed. By integration of the knowledge learned from those of *Mycobacterium tuberculosis* and *S. coelicolor*, the conserved Asp site of actinomycete GlnR is proved unphosphorylated but critical for homodimerization *via* its charge interactions with the surrounding residues, which in turn, is essential for its physiological function *in vivo* and DNA binding ability *in vitro*.

EXPERIMENTAL PROCEDURES

Bacterial strains, Plasmids and Growth conditions— *Escherichia coli* strains were grown at 37 ^{o}C in Lysogeny broth (LB) medium (26). *A. mediterranei* were grown at 30 ^{o}C in the nutrient-rich Bennet medium (27), To examine the growth phenotypes of *A. mediterranei* U32 and its *glnR* mutants, strains were incubated at 30 ^{o}C in minimal medium (MM) (27) supplemented with 80 mM potassium nitrate or 60 mM ammonium sulfate as the sole nitrogen source, and the growth was observed after 7 days' cultivation. *S. coelicolor* M145 and its derivatives were generally cultured at 30 ^{o}C in the MS medium for spore suspension preparations (28), while phenotype analysis was observed in nitrogen-limited N-Evans medium with 5 mM nitrate or 100 mM ammonium sulfate as the sole nitrogen source after 4 days'cultivation. If necessary, the media were supplemented with antibiotics (100 μg ml^{-1} for ampicillin, 50 μg ml^{-1} for kanamycin, 50 μg ml^{-1} for apramycin and 50 μg ml^{-1} for thiostrepton).

Expression and Purification of GlnR Regulatory Domain (*GlnRRec*) *protein*—DNA fragments encoding the receiver domains of GlnR proteins were PCR-amplified using the genomic DNA of *A. mediterranei* U32 (*AmeglnRRec*) and *M. tuberculosis* H37Rv (*MtbglnRRec*). The PCR products were digested and inserted into the pET28b expression vector resulting in N-terminal 6×His tagged pET-28bAmeglnRRec and pET-28bMtbglnRRec. The plasmid was transformed into *E. coli* BL21 (DE3) strain (Novagen) and the cells were cultured at 37 °C in LB medium containing 50 μg ml^{-1} kanamycin. Protein expression was induced by adding IPTG (isopropyl β-D-thiogalactoside) into the medium to a final concentration of 1 mM when the OD600 is 0.8. Then the cells were harvested by centrifugation at 5000 g for 10 min at 4 °C, resuspended in a lysis buffer (50 mM Tris-HCl, pH 8.0, 100 mM NaCl and 1 mM PMSF), and disrupted using a French Press. The recombinant protein was purified with affinity chromatography using Ni^{2+}-NTA (Ni^{2+}-nitrilotriacetate) superflow column (Qiagen) pre-equilibrated with buffer A (50 mM Tris-HCl, pH 8.0 and 100 mM NaCl) and then washed with buffer B (buffer A supplemented with 50 mM imidazole) to remove nonspecific binding proteins. The target protein was eluted with buffer C (buffer A supplemented with 250 mM imidazole), and the eluted fractions was further purified using a gel-filtration column (GE-healthcare). After the two-step purification, the target protein was of sufficient purity (above 95%)

and was then concentrated to approx. 10 mg ml^{-1} in buffer A by ultrafiltration for further structural and biochemical studies.

Selenomethionine-substituted AmeGlnRRec protein was prepared following a method described previously (29). Purification of the selenomethionine AmeGlnRRec protein was performed using the same methods as for the native protein. Gel-filtration analysis of the purified protein was performed to measure the oligomeric state of AmeGlnRRec in solution. The high and low molecular weight (mass) Calibration Kits (GE-Healthcare) were used to calibrate the molecular mass of wild-type and mutants of AmeGlnRRec. All the above analysis was carried out on an FPLC system (GE-healthcare). Protein samples of 100 µl each were loaded into a 0.5 ml sample loop and injected into a Superdex 200 column. The apparent molecular mass of the protein sample was calculated according to the protocol provided in the kit.

Phos-tag acrylamide gel analysis of GlnR phosphorylation—Sample preparation for *in vivo* detection of phosphorylation, standard protocol was used with minor modifications (30). *A. mediterranei* U32 or *S. coelicolor* M145 and related mutants were grown in Bennet or MS medium [10] at 30 ^{o}C for 2 days and were then harvested by swabbing from the plate. Aliquots of the cells were washed and resuspended in MM or N-Evans medium supplemented with 80 mM potassium nitrate or 60 mM ammonium sulfate as the sole nitrogen source for GlnR or with 4 mM or 0 mM potassium hydrogen phosphate as the sole phosphate source for AmePhoP. After 12 h of growth, cells were pelleted by centrifugation, immediately following harvest; cells were lysed with 3.3 ml of 1 M formic acid (0.55 M final concentration formic acid) per equivalent of pellet of 50 ml of 0.2 OD600 of cells. French press was used to lysate the frozen cell pellet. Each lysate was solubilized by the addition of 200 µl 5 M NaOH (0.17 M final concentration) to neutralize the solution and 1.5 ml 5xSDS loading solution. Resulting cell lysates (20 µl) were immediately loaded onto a Phos-tag gel for electrophoresis as described below, the whole lysis process should keep low temperature to prevent the hydrolysis of phosphor-Asp residues.

For *in vitro* phosphorylation experiments, solutions of 10 µM protein in phosphorylation buffer (50 mM Tris-HCl, pH 8.0, 100 mM NaCl, 2 mM β-mercaptoethanol, 20 mM $MgCl_2$) with or without incubation with 20 mM ammonium hydrogen phosphoramidate (synthesized as described previously (31) for 30 min at 37 °C were prepared. The phosphorylation reactions were stopped by addition of 5xSDS-loading buffer. Phos-tag acrylamide gels were prepared as previously described with minor modifications (30,32,33). Phos-tag acrylamide running gels contained 12% (w/v) 29:1 acrylamide: N, N-methylene-bis-acrylamide, 375 mM Tris, and pH 8.8, 0.1% (w/v) SDS. Gels were copolymerized with 25 µM Phos-tag acrylamide and 50 µM $MnCl_2$ for analysis of purified GlnR and other positive control proteins. The stacking gels contained 5% (w/v) 29:1 acrylamide: N, N-methylene-bis-acrylamide, 125 mM Tris, and pH 6.8, 0.1% (w/v) SDS. All Phos-tag acrylamide-containing gels were run at 4 ^{o}C under constant voltage (120 V). Gels were fixed for 10 min in standard transfer buffer, 20% (v/v) methanol, 50 mM Tris-HCl, 40 mM glycine, with 1 mM EDTA added to remove Mn^{2+} and then incubated for an additional 20 min in transfer buffer without EDTA to remove the chelated metal. Transfer to nitrocellulose membranes was performed using a Bio-Rad transfer apparatus under a constant 300 mA for 1 h. Western blotting assay was performed using standard protocols.

Crystallization, Data collection and Structure determination—The AmeGlnRRec and MtbGlnRRec proteins were used in crystallization experiments at 4 °C using the sitting-drop vapour-diffusion method. Crystals were grown in the drop containing equal volumes (1 µl) of the protein solution (approx. 10 mg/ml AmeGlnRRec/MtbGlnRRec) and the reservoir solution (0.1 M Tris-HCl, pH 8.0 and 20% MPD), (1.8 M sodium acetate trihydrate, pH 7.0, 0.1 M Bis-Tris propane), respectively. For diffraction data collection, the AmeGlnRRec and MtbGlnRRec crystals were first cryo-protected using paratone oil (Hampton Research) and then flash-cooled in liquid nitrogen. Selenium SAD (single-wavelength anomalous dispersion) and native data of AmeGlnRRec were collected to

resolution of 3.0 Å and 2.8 Å respectively from flash-cooled crystals at 100 K at the Shanghai Synchrotron Radiation Facility (SSRF, China), beamline BL17U. The native data of MtbGlnRRec was collected to 2.8 Å. The diffraction data were processed, integrated and scaled together using the HKL2000 suite.

Structure of the AmeGlnRRec was solved using the Autosol implemented in Phenix (34). Over 60% main chain residues were built and the overall figure-of-merit was increased from 0.35 to 0.69 at 3.0 Å. The full-structure model was built manually using the program Coot (35). Structure refinement was carried out using Phenix and refmac. Since the resolution and statistics of SAD data set of AmeGlnRRec is better than the native data, the SAD data set was used in the final refinement of the structure of AmeGlnRRec. The structure of MtbGlnRRec was solved by molecular replacement using the structure of AmeGlnRRec as a starting model. The final model was refined to 2.8 Å. All the statistics of data collection and structure refinement are summarized in **Table 1**.

Molecular Dynamic Simulations—The starting structure of AmeGlnR monomer was extracted from the crystal structures of AmeGlnR dimer. The D50A, D50E and D50N mutants were built from the wild type by mutating the Aspartic acid into Glutamate or Asparagine, respectively. After that, each system was solvated by TIP3P waters with 0.15 M NaCl. Finally, each simulation system includes about 17,000 atoms (55 Å × 55 Å × 55 Å).

MD simulations were carried out with the GROMACS 4.6.1 package with NPT ensemble and periodic boundary condition (36). The AMBER99SB-ILDN force field was applied for the simulations (37). Energy minimizations were first performed to relieve unfavorable contacts, followed with 2 ns in total to equilibrate the side chains of protein and solvent. The particle-mesh Ewald method was used for long-range electrostatic interactions with a short-range cutoff of 1.2 nm. All simulations were run at 300 K using the v-rescale method with a coupling time of 0.1 ps (38). The pressure was kept at 1 bar using the Berendsen barostatτp=1.0 ps and a compressibility of 4.5×10-5 bar-1. SETTLE constraints and LINCS constraints were applied on the hydrogen-involved covalent bonds in water molecules and in other molecules respectively, and the time step was set to 2 fs. Each system was put into a 150 ns production run.

Electrophoretic Mobility Shift Assay (*EMSA*)—For expression of recombinant mutated AmeGlnR (*i.e.*, D50A, D50N, T9A, R52A, T9A/R52A, R111A and R111E mutants), the wild type *AmeglnR* gene on the expression plasmid pET28b was mutated using site-directed mutagenesis methods (18). The *glnA* promoter region of *A. mediterranei* U32 was generated by PCR and was then inserted into the *Hinc*II site of pUC18. The obtained plasmid was used as the template for preparation of the FAM-labeled probes using the universal primer pair of FAM-labeled M13F (-47) and M13R (-48). FAM-labeled probe (30 ng) was incubated with varying amounts of AmeGlnR or its mutants at 25 °C for 20 min in a buffer of 25 mM Tris-HCl (pH 8.0), 50 mM KCl, 2.5 mM $MgCl_2$, 5% glycerol, 1 mM dithiothreitol (DTT) and 100 μg ml^{-1} sonicated salmon sperm DNA (Sangon) (total volume 20μl). As GlnR has been proved a specific regulator for binding of the *glnA* promoter region in *A. mediterranei* U32 (39) and the EMSA employed in this study is to measure the DNA binding affinities of GlnR as well as its mutants, the cold probe competition assay was unnecessary and was therefore omitted. The resulting DNA-protein complexes were subjected to electrophoresis on agarose gels with a running buffer containing 40 mM Tris-HCl (pH 7.8), 20 mM boric acid, and 1 mM EDTA at 150 V and 4 °C for 1 h. After electrophoresis, gels were directly scanned for fluorescent DNA using an ImageQuant™ LAS 4000 (GE healthcare).

Complementation Assay—The *A. mediterranei glnR* gene together with its native promoter region was amplified from *A. mediterranei* genome DNA, and ligated with pRT803 which was excised by EcoRV, yielding plasmid pRT803AmeglnR, which was then used as the template for site-directed mutagenesis of *AmeglnR*. After verified by DNA sequencing, the complementation plasmids were transformed into *A. mediterranei* U32Δ*glnR* using Bio-Rad Gene pulser according to the methods described by (40). Transformants were selected in Bennet agar plates containing hygromycin. The *S. coelicolor glnR* gene together

with its native promoter region was excised from pSETScoglnR with BamHI (18) and was subsequently cloned into the same site of pBluescript II SK (Stratagene), yielding plasmid pSKScoglnR, which was then used as the template for site-directed mutagenesis of *scoglnR*. The generated plasmids with various mutations of *scoglnR* were digested with BamHI and inserted into the same site of pSET1521 (41) to obtain the relevant plasmids for *scoglnR* complementation. After being verified by DNA sequencing, the complementation plasmids were conjugated into *S. coelicolor* M145Δ*glnR* (18). Exconjugants were selected by growth on MS agar flooded with nalidixic acid and thiostrepton.

In vivo *Chemical Cross-linking Experiment*—*A. mediterranei* strains containing the mutated residues in *glnR* were made by complementing the *A. mediterranei* U32Δ*glnR* strain with mutated *A. mediterranei glnR* fused with a Flag tag at the C terminus using the method described above. *A. mediterranei* was firstly cultured in liquid Bennet medium at 30 °C for 48 h before being inoculated into fresh liquid Minimal medium supplemented with either 80 mM KNO_3 or 60 mM $(NH_4)_2SO_4$ for another 24 h culture. Cells were then collected and the cell pellets were re-suspended in PBS and exposed to 5 mM DSS (Pierce). After 20 min incubation at 25 °C, the reaction was quenched with the addition of 50 mM Tris-HCl (pH 8.0) (final concentration) for 15 min. The samples were subjected to SDS-PAGE and immunoblot assays were performed using the anti-Flag antibody.

Reverse Transcription PCR (*RT-PCR*)—For RNA extraction, wild type *A. mediterranei* U32 and *glnR mutants* were grown in liquid Bennet medium for 48 h before being inoculated into fresh liquid Bennet medium supplemented with 80 mM KNO_3 or 60 mM $(NH_4)_2SO_4$ for further culture for 36 h. Total RNA was extracted using TRIzol reagent (Invitrogen). RNA was treated with RNase-free DNase I (Promega) to prevent contamination of trace genomic DNA. Reverse transcription was performed with a random hexamer primer using 3 μg RNA in a total volume of 30 μl employing Super-Script III reverse transcriptase (Invitrogen). PCR was performed employing 20 ng reaction mixtures as the template to check the transcription of *nasA* and *glnR* genes and using the *rpoB* gene as the internal control. A negative control was made by following the same procedures except that the addition of reverse transcriptase was omitted. Two independent samples were used for analyses.

Results

***GlnR of Either* A. mediterranei *or* S. coelicolor *Is Unphosphorylated at the Potential Asp Phosphorylation Site*—** Since the Phos-tag methods (30,32,33) are able to characterize the phosphorylation state of the Asp residues in typical RRs such as that shown for PhoB from *E. coli* (EcoPhoB) cell lysates (42), similar *in vitro* phosphorylation assays employing the high-energy phospho-donor, ammonium hydrogen phosphoramidate (PA) against the purified recombinant proteins of AmeGlnR and ScoGlnR proteins were conducted individually. Both of the annotated typical RRs, *i.e.*, PhoP of *A. mediterranei* (AmePhoP) (13) and SCO5403 of *S. coelicolor* (21) bearing the highly conserved acidic quintet in their amino acid sequences, as well as the purified well-characterized EcoPhoB could be successfully phosphorylated *in vitro* by PA, likely at their corresponding Asp residues, while neither AmeGlnR nor ScoGlnR could (**Figure 1A**). Therefore, it is unlikely that the conserved Asp residues of either of the two GlnRs can be phosphorylated by the high energy phosphodonor *in vitro*.

In order to test whether GlnR is phosphorylated or not *in vivo*, the phosphorylation status of AmeGlnR or ScoGlnR *in vivo* is tested *via* western blot analysis against the cell lysates of *A. mediterranei* or *S. coelicolor* electrophoresed on Phos-tag gel, employing AmePhoP as a positive control and AmePhoP(D52A) as a negative control. In accord with the fact that the Asp52 of PhoP is phosphorylated under the phosphate limitation conditions (43), AmePhoP exhibits a single band on the gel when cells are grown in phosphate (K_2HPO4) rich medium, whereas double bands of AmePhoP are observed for cells grown in phosphate-limiting media. Obviously**,** the upper band corresponding to the phosphorylated AmePhoP disappears in the D52A mutation, indicating that Asp52 is the phosphorylation site (**Figure 1B**). In contrast, although GlnR is

functional under nitrogen limited conditions (39), no phosphorylation band of AmeGlnR or ScoGlnR can be observed in lysates of cells grown in either nitrogen rich ($(NH_4)_2SO_4$) or nitrogen limited (KNO_3) media. All of these results are in good consistence with the results of the *in vitro* experiments mentioned above (**Figure 1A**), and therefore, we conclude that both AmeGlnR and ScoGlnR are unphosphorylated at their conserved Asp residues.

Crystal Structures of the GlnR Receiver Domains from* A. mediterranei *and* M. tuberculosis *Are Distinct from That of the Typical RRs Regarding to the Potential "Phosphorylation Pocket" and Its Surrounding Amino Acid Residues— We determined the crystal structures of the receiver domains of GlnR from *A. mediterranei* U32 (AmeGlnRRec) and *M. tuberculosis* (MtbGlnRRec). The final structure models of both proteins are refined to 2.8Å, with their statistics summarized in **Table 1**. Considering that AmeGlnRRec and MtbGlnRRec not only share 58% sequence identity (**Figure 2A**), but also form similar homodimer structures (r.m.s.d=1.0Å), AmeGlnRRec alone is selected for further structural and functional analyses. (**Figure 2B)** (The structures of AmeGlnRRec and MtbGlnRRec have been deposited to Protein Data Bank with the code: 4O1H and 4O1I, respectively.)

The structure of AmeGlnRRec consists of five alternating β-strands and α-helices folding into a five-stranded parallel β-sheet in the middle surrounded by two α-helices on one side and three on the other (**Figure 2B**), which is similar to most of the known structures of the typical RR receiver domains (22) except that the helices α1, α2 and α4 of AmeGlnRRec are partially unwound (**Figure 2C**). We notice that the so called "phosphorylation pocket" defined in the typical RRs as well as its microenvironment are significantly altered in the structure of AmeGlnRRec (**Figure 2A** and **Figure 2C**). All of the five residues essential for the phosphorylation of PhoB except Asp50 are neither conserved nor in proper position, which is also demonstrated by the structural-based sequence alignment among GlnR proteins from representative actinomycetes and the well-characterized typical and atypical RRs from Gram-negative bacteria (**Figure 2A**). The Glu9 and Asp10 residues known to bind with Mg^{2+} to promote phosphorylation and dephosphorylation in PhoB of *E. coli* are replaced by residues Thr9 and Ala10 in AmeGlnRRec, respectively. These changes are likely to exclude the binding of a divalent metal cation, and hence reduce the possibility of phosphorylation at AmeGlnRRec residue Asp50. In addition, the Thr and Lys residues believed to communicate between the phosphorylation site and dimer interface in typical RRs are changed to Val81 and Leu100, respectively, and the critical conformation switch residue Tyr is also substituted with an Ile98 in AmeGlnRRec. These data suggest that the AmeGlnR is significantly diverged from the canonical RRs with respect to the potential "phosphorylation pocket" and its surrounding amino acid residues.

When the monomer structure of AmeGlnRRec is superimposed with that of the phosphorylated PhoB (r.m.s.d=2.1Å), we find that the β1-α1 and β3-α3 loops move towards the putative phosphorylation pocket, thus shrinks the size of the "pocket". It is particularly significant that the Arg52 residue, conserved among all GlnR proteins but completely different in Gram-negative OmpR/PhoB subfamily proteins (**Figure 2A**), protrudes from the β3-α3 loop into and occupied the "pocket" with its guanidinium side chain positioned at the close vicinity of the carboxyl side chain of the only conserved Asp50. Based on the measured distance of the interactions, an ionic bridge may form between the side chains of these two residues and the side chain of Asp50 may further be stabilized by forming another hydrogen bond with Thr9. Thus, the configuration of Arg52 not only lessens the likelihood of residue Asp50 being phosphorylated but also introduces a hydrogen-bonding/ionic interaction network, which may provide an alternative mechanism for maintaining the homodimerization status of GlnR different from that of Asp phosphorylation in typical RRs **(Figure 2C).**

Homodimerization of the Two GlnR Monomers through Their α4-β5-α5 Interface Is Essential for Its Physiological Function—The crystal structure data suggest that both AmeGlnRRec and MtbGlnRRec form homodimers. The interface involves the α4-β5-α5 secondary

structure elements from both monomers and buries about 30% of the total surface area, which is similar to that of the phosphorylated typical RRs, such as PhoB and ArcA **(Figure 3A** and **Figure 3B**), where homodimerization through such kind of interface is universal and essential for their physiological activities. On the other hand, in contrast to ArcA and PhoB, there is lower percentage of hydrophilic residues but higher percentage of hydrophobic residues within the interface of the two GlnR monomers, presumably favors tighter protein-protein interactions **(Figure 3A).** The Arg111 residue in AmeGlnRRec from β5 of both monomers A and B, conserved among almost all OmpR/PhoB subfamily proteins except for the atypical ChxR from *Chlamydia trachomatis* **(Figure 2A),** is found stacking against each other by π-π interactions. This Arg residue further stabilizes the interface by forming salt-bridge and hydrogen-bond networks with Asp97 and Glu107 from both monomers **(Figure 3C).** The predominant role of this Arg residue in maintaining the homodimer is confirmed by site-directed mutagenesis analysis followed by gel filtration verification, in which an R111A single mutation results in a disruption of the homodimer of AmeGlnRRec **(Figure 3D).** The hydrophilic interactions among Arg111,Asp97 and Glu107 are surrounded by hydrophobic residues Leu86, Val89, Ile98, Ala106, Ala110 and Leu114 protruded from α4 and α5 helices of monomers A and B, strengthening the homodimer interaction **(Figure 3A** and **3C**).

The dimerization and extensive interactions of the receiver domains infer that GlnR may form a homodimer as its functional status under physiological conditions. However, we failed in crystallization and analyzing the oligomeric state of the full length GlnR using the heterogeneously expressed protein probably due to its aggregation in solution. Alternatively, as shown in **Figure 4,** we demonstrate that the AmeGlnR protein exists mainly as dimers *in vivo* in the presence of cross-linking agent DSS under either nitrogen-rich or limited conditions. We further explore whether the α4-β5-α5 interface is essential for the homodimerization of full length AmeGlnR. Indeed, AmeGlnR harboring a R111A mutation changes the oligomeric state from dimers to monomers, which suggests that the homodimerization of AmeGlnR is dependent on the α4-β5-α5 interface *in vivo* **(Figure 4).**

The *glnR* null mutants of both *A. mediterranei* U32 and *S. coelicolor* are proved unable to grow on minimal medium when nitrate is supplied as the sole nitrogen source (10,39). Similar growth failure was observed when mutations of R111A/E **(Figure 5)** or R108A/E (data not shown) were introduced individually into *AmeglnR* or *ScoglnR*, respectively**.** Consistent with these physiological phenotypes, the transcription of GlnR target genes, such as *nasA* and *glnA*, are not activated in *A. mediterranei glnR*(R111A/E) mutants either **(Figure 6)**. Further EMSA experiments using purified mutated proteins indicated that the DNA binding ability of AmeGlnR(R111A) and AmeGlnR(R111E) proteins were all significantly reduced **(Figure 7).** These data suggest that the homodimer formation through the α4-β5-α5 interface is indispensable for GlnR function *in vivo*, and the disruption of homodimer formation of GlnR may lead to the impairment of its DNA-binding ability, therefore abolishing the regulatory function of GlnR.

The Conserved Asp50 of GlnR Is Critical for Maintaining the Receiver Domain-mediated Protein Dimerization and the Corresponding Physiological Function— The above biochemical and structural analyses clearly demonstrate that GlnR with the conserved Asp unphosphorylated is functional. However, since the D50A mutation supposed to mimick its unphosphorylated status of GlnR can neither complement for the growth defect of the *glnR* null mutants nor bind to its target promoter such as that of *glnA* **(Figure 5** and **Figure 7** and refer to Jenkins *et al.*, 2012 for the data of *M. smegmatis*), the underlying mechanism for the importance of Asp50 in maintaining the biological function of GlnR needs to be addressed.

The crystal structure of the wild type AmeGlnRRec protein indicates that Asp50 forms an ionic interaction with Arg52 and a hydrogen bond with Thr9 (**Figure 2C** and refer to the third section of ***Results***). This is also true in the structure of MtbGlnRRec, in which, Asp49 forms similar interactions with Arg51 and Thr8. Therefore, we propose that these charge interactions may stabilize the homodimeric

conformation of GlnR **(Figure 2C),** and D50A mutation in AmeGlnR may completely disrupt these interactions and thus result in dismantling the functional homodimerization.

The influence of this D50A mutation upon homodimer formation of either the AmeGlnRRec or the full-length AmeGlnR protein was verified using *in vitro* size-exclusion chromatographic analysis or *in vivo* chemical crosslinking assay, respectively. Both results suggest that while the wild type AmeGlnR forms homodimer, AmeGlnR(D50A) exists mainly as monomers **(Figure 3D** and **Figure 4).** To explore the possible mechanism underlying the effect of the D50A mutation upon dimerization, the structure of AmeGlnRRec(D50A) is modeled based on that of the wild type AmeGlnRRec through molecular dynamic (MD) simulations (**Figure 8)**. Comparing these two structural models, it is obvious that the Asp50-focused charge interaction network (with Arg52 and Thr9) is completely abolished in the D50A mutant, which may cause both the Arg52 residue and the β3-α3 loop (residues Ala50-Asp54) move away from the so called 'phosphorylation pocket', leaving a space to accommodate the β4-α4 loop (residues Val81-Val86) shifted away from the dimer interface (shown as arrows in **Figure 8**). The conformational change in β4-α4 loop and the connecting α4 helix may greatly impair the α4-β5-α5 interface, through which the two monomers form a homodimer.

To further verify the above hypothesis, we generated two groups of mutants based on the structural information. The *AmeglnR*(D50N) and *AmeglnR*(D50E) mutants are designed to maintain the hydrogen bonds of either Asn50 or Glu50 with Arg52 and Thr9 although the interactions are weakened due to the loss of the proposed salt bridge or varied the bond-lengths in between. The AmeGlnR mutants containing either R52A or T9A alone and the double mutant of R52A/T9A belong to the second group, which is designed to test the effect of charge interactions by altering the surrounding amino acid residues individually or together rather than simply mutating the Asp50 residue as in the first group.

All of these mutants were tested for their *in vivo* oligomeric status, growth properties and *in vitro* DNA binding capabilities. The AmeGlnR containing the single mutation of D50N or D50E or R52A or T9A alone still forms a homodimer, while the GlnRs with either a single mutation of D50A or double mutation of T9A/R52A exist as monomers *in vivo* **(Figure 4).** Consistently, the AmeGlnR proteins containing D50N or D50E or R52A or T9A mutation individually can bind to the *glnA* promoter *in vitro* and activate its transcription *in vivo*, while the D50A or T9A/R52A mutated AmeGlnR cannot **(Figure 6** and **Figure 7).** Physiologically, as expected, the mutants of D50N or D50E or R52A or T9A alone can complement the growth defect of the Δ*glnR* host on minimal medium supplemented with nitrate as the sole nitrogen source **(Figure 5)**, but neither AmeGlnR(D50A) nor AmeGlnR(R52A/T9A) mutant can. In addition, the AmeGlnR(D50L) mutant, which diminishes the charge interaction completely as that of D50A mutant but maintains the length of the side chain similar to that of Asp, is shown to completely impair the complementation function either (data not shown). It is also significant that similar results are obtained in *S. coelicolor* with corresponding mutations in ScoGlnR (data not shown). All of the above data suggest that the charge interactions among Asp50, Arg52 and Thr9 of AmeGlnR are critical for maintaining its receiver domain-mediated protein dimerization and the corresponding physiological function, which may be applied to the GlnRs of other actinomycetes.

Discussion

The global transcription factor GlnR of the Gram-positive actinomycetes has been one of the major research focuses with respect to bacterial molecular physiology. It is due to not only its pivotal role in coordinating the expression of genes related to nitrogen metabolism of this industrially and medically important bacterial clade in response to the environmental nitrogen conditions, but also its significantly different mode of action as an orphan RR in contrast to that of the well-studied TCS in Gram-negative enteric bacteria. However, the progress of the research has been largely hindered by the difficulties lined in biochemical determination and genetic

characterization of GlnR phosphorylation status and its impact upon the protein's structure-function relationship under different physiological conditions. In this study, with a great deal of technology improvement, taking the advantage of both the comprehensive research system developed in *A. mediterranei* and the highly conserved properties of GlnR from *S. coelicolor* and *M. tuberculosis*, multilevel evidence is gathered to support the conclusion that the actinomycete GlnR is an atypical OmpR/PhoB subfamily RR and functions as a homodimer stabilized by the critical charge interactions of the unphosphorylated conserved Asp residue with its spatially nearby polar amino acid residues.

Because the universal presence of a so-called "phosphorylation pocket" within the N-terminal receiver domain of the typical RRs, RRs without the pocket, usually determined by sequence alignment, are categorized "atypical" subject to various regulatory mechanisms different from that of phosphorylation at the conserved Asp residue in the "pocket" region (44). The crystal structures of AmeGlnRRec and MtbGlnRRec and the structural-based sequence alignment analysis presented in this study demonstrate that the actinomycete GlnR not only lacks the typical acidic pocket but also has the possibility of phosphorylation at the conserved Asp50 site being spatially excluded (**Figure 2**). Therefore, in combination with the reproducible negative results in detecting the phosphorylated GlnR either *in vitro* or *in vivo* along with the clear positive controls**,** it is quite sure that the functional GlnR is not phosphorylated at its conserved aspartate residue (**Figure 1**). However, this residue is still essential for the physiological function of AmeGlnR as shown both *in vitro* and i*n vivo* in this study (**Figure 5**).

Usually the Glu/Ala mutation at the conserved phospho-accepting Asp residue is known to mimic the phosphorylation/unphosphorylation status of the RRs (45,46) while exceptions do exist. For instance, the Asp→Glu mutant of VirG, an RR of the VirA/VirG two-component system in *Agrobacterium tumefaciens*, does not mimic the phenotype of the phosphorylated VirG. In fact, this study offers another case, where, in contrast to the completely deficient GlnR(D50A) mutant, the GlnR(D50N) is still functional, which is another frequently used mimetic model for the unphosphorylated status. Therefore, these mutations are useful models for mechanistic studies rather than for the proof of the presence of phosphorylation.

The current understanding of the mechanism of activation of the typical RRs is derived from comparisons of structures under the phosphorylated *versus* the unphosphorylated states (3,8). For most of the typical RRs, the phosphorylation at their Asp residues induces conformational changes. Particularly, the reorientation of β4-α4 loop and the two conserved switch residues, namely Ser/Thr from β4 and Tyr/Phe from β5, are changed to facilitate the transition of the RR from monomers (47-49) or weak dimers (2), both at their unphosphorylated states, to the "tight" functional homodimers through the formation of a common α4-β5-α5 ionic interface contributed by a set of highly conserved residues. This strong interaction further brings the DNA binding domains into close proximity, allowing them to bind to the direct repeat half-sites that comprise the recognition sequences for most OmpR/PhoB subfamily RRs (3,50). On the other hand, the crystal structure of the orphan RR GlnR, unphosphorylated at the conserved Asp residue, forms a functional homodimer through the α4-β5-α5 interface, which is in accordance with the previous data regarding the GlnR binding consensus sequences where two GlnR binding boxes are found in many cases (18,51).

Various mechanisms are adopted for facilitating and stabilizing the functional dimerization in atypical RRs in addition to the universal α4-β5-α5 secondary structure element critical for a proper interface. First of all, both ionic and hydrophobic interactions within the dimer interface are employed as the main forces for stabilizing the functional dimer. In the cases of HP1043 from *Helicobacter pylori* and ChxR from *C. trachomatis*, no matter the conserved Arg residue (corresponding to Arg111 of AmeGlnR) is present in the former or absent in the latter**,** they all retain the conserved Tyr residues as in typical RRs as well as a few atypical RRs **(Figure 2A),** and the side chains in both cases adopted a similar

orientation towards the active site as that of the phosphorylated typical RRs in order to facilitate the formation of active dimers. In contrast, the α4 helix of AmeGlnRRec is partially unwound and the residues corresponding to Ser/Thr and Tyr/Phe in typical RRs are replaced by Val81 and Ile98, with the side chains of which adopt similar orientations as that of the unphosphorylated typical RRs **(Figure 9).** However, the smaller side chain of Ile98, comparing to that of Tyr/Phe, may allow a close interaction between the two monomers through the α4-β5-α5 interface, which is highly similar to that of the phosphorylated typical RRs. In fact, similar small side chain residues are found in the GlnR proteins from various actinomycetes **(Figure 2A),** which suggests that a dimer stabilizing mechanism distinct from that of HP1043 and ChxR is commonly adopted.

More significantly, along with resolving the controversial mutational analysis upon the conserved Asp residue within the missing "phosphorylation pocket" quintet of actinomycete GlnR, this study demonstrates that this Asp residue plays an important role in maintaining the functional conformation of the active homodimer via formation of salt bridge/hydrogen-bonds interactions with two spatially close Arg and Thr residues (T9-D50-R52 interactions)**.** This unique mechanism, novel among all of the atypical RRs studied so far, is comprehensively verified by mutational analysis detecting their dimerization capabilities as well as related functional impacts both *in vitro* and *in vivo***.** In addition, the MD simulation for wild type and all of the mutants indicates that a significant conformational difference occurs in the β4-α4 loop is only observed in the GlnR(D50A) (**Figure 8)** and GlnR(D50L) (data not shown) mutants, where the loop shifts toward the D50 position and may consequently influence or even disable the homodimerization of GlnR *via* weakening the α4-β5-α5 dimer interface. Interestingly, upon phosphorylation/dephosphorylation, the β4-α4 loop of the typical PhoB actually undergoes significant rearrangement, changing PhoB from homodimers to monomers, respectively. The spatial position of the loop in the unphosphorylated PhoB is the same as that in GlnR(D50A) (3), which may therefore explain the negative effect of D50A mutation upon the oligomerization of GlnR.

So far, this study has shown that the actinomycete GlnR is not phosphorylated at the conserved Asp residue *in vitro* or *in vivo* and thus confirmed to be an atypical RR. Further RT-PCR analyses employing two GlnR target genes, *nasA* and *glnA* show that the transcriptional activation ability of the AmeGlnR mutants is consistent with their corresponding growth phenotypes (**Figure 6**), *i.e*., the active GlnR mutants, GlnR(D50E), GlnR(D50N), GlnR(T9A) and GlnR(R52A) are still able to respond to the extracellular nitrogen availabilities while the inactive GlnR mutants, GlnR(D50A), GlnR(T9A/R52A) and GlnR(R111A/E) are not.

It is known that apart from the possible post-translational modification, transcription of *S. coelicolor glnR* gene is stringently regulated by the environmental nitrogen availability (10), which may alter the quantity of functional GlnR available *in vivo*. However, the expression of *glnR* in *A. mediterranei* and *M. smegmatis* is not significantly affected by the extracellular nitrogen sources (15 ,25). Considering the fact that the biological function of the above GlnRs is only found in nitrogen limited conditions, at least GlnRs of *A. mediterranei* and *M. smegmatis* are expected to be regulated by uncharacterized mechanisms, most likely post-translational modification, resulting in distinct activities in GlnR-mediated global transcriptional regulation. Although eukaryotic phosphorylation on Ser, Thr or Tyr residues, often identified in prokaryotic proteins (52), are seemingly excluded by the Phos-tag assays under our tested conditions, in addition to that of Asp residue, they might occur under other cultural conditions or detected by other assay methods. Meanwhile, other types of modifications besides phosphorylation have been reported to alter the activities of atypical RRs, *e.g.* posttranslational acetylation of RcsB (53,54), and binding of the small ligand Jadomycin B in the modulation of the JadR1 from *Streptomyces venezuelae* (44). Interestingly, in the above mentioned two cases, although different mechanisms are adopted, they both inactivate rather than activate the atypical transcription factors under certain metabolic

conditions. In the case of actinomycete GlnR, which is naturally active in its dimer status that is stabilized by a robust charge interaction network, "activation" of GlnR seems unnecessary while similar "inactivation" consequence conveyed by its special regulation mechanism(s) is expected under nitrogen-rich conditions. Therefore, efforts are currently undertaking in that direction.

REFERENCE

1. Stock, A. M., Robinson, V. L., and Goudreau, P. N. (2000) Two-component signal transduction. *Annu. Rev. Biochem.* **69**, 183-215
2. Gao, R., and Stock, A. M. (2009) Biological insights from structures of two-component proteins. *Annu. Rev. Microbiol.* **63**, 133-154
3. Bachhawat, P., Swapna, G. V., Montelione, G. T., and Stock, A. M. (2005) Mechanism of activation for transcription factor PhoB suggested by different modes of dimerization in the inactive and active states. *Structure* **13**, 1353-1363
4. Jeon, Y., Lee, Y. S., Han, J. S., Kim, J. B., and Hwang, D. S. (2001) Multimerization of phosphorylated and non-phosphorylated ArcA is necessary for the response regulator function of the Arc two-component signal transduction system. *J. Biol. Chem.* **276**, 40873-40879
5. Chen, Y., Birck, C., Samama, J. P., and Hulett, F. M. (2003) Residue R113 is essential for PhoP dimerization and function: a residue buried in the asymmetric PhoP dimer interface determined in the PhoPN three-dimensional crystal structure. *J. Bacteriol.* **185**, 262-273
6. Mack, T. R., Gao, R., and Stock, A. M. (2009) Probing the roles of the two different dimers mediated by the receiver domain of the response regulator PhoB. *J. Mol. Biol.* **389**, 349-364
7. Hong, E., Lee, H. M., Ko, H., Kim, D. U., Jeon, B. Y., Jung, J., Shin, J., Lee, S. A., Kim, Y., Jeon, Y. H., Cheong, C., Cho, H. S., and Lee, W. (2007) Structure of an atypical orphan response regulator protein supports a new phosphorylation-independent regulatory mechanism. *J. Biol. Chem.* **282**, 20667-20675
8. Kern, D., Volkman, B. F., Luginbuhl, P., Nohaile, M. J., Kustu, S., and Wemmer, D. E. (1999) Structure of a transiently phosphorylated switch in bacterial signal transduction. *Nature* **402**, 894-898
9. Amon, J., Titgemeyer, F., and Burkovski, A. (2010) Common patterns - unique features: nitrogen metabolism and regulation in Gram-positive bacteria. *FEMS. Microbiol. Rev.* **34**, 588-605
10. Tiffert, Y., Supra, P., Wurm, R., Wohlleben, W., Wagner, R., and Reuther, J. (2008) The *Streptomyces coelicolor* GlnR regulon: identification of new GlnR targets and evidence for a central role of GlnR in nitrogen metabolism in actinomycetes. *Mol. Microbiol.* **67**, 861-880
11. Malm, S., Tiffert, Y., Micklinghoff, J., Schultze, S., Joost, I., Weber, I., Horst, S., Ackermann, B., Schmidt, M., Wohlleben, W., Ehlers, S., Geffers, R., Reuther, J., and Bange, F. C. (2009) The roles of the nitrate reductase NarGHJI, the nitrite reductase NirBD and the response regulator GlnR in nitrate assimilation of *Mycobacterium tuberculosis*. *Microbiology* **155**, 1332-1339
12. Tullius, M. V., Harth, G., and Horwitz, M. A. (2003) Glutamine synthetase GlnA1 is essential for growth of *Mycobacterium tuberculosis* in human THP-1 macrophages and guinea pigs. *Infect. Immun.* **71**, 3927-3936
13. Zhao, W., Zhong, Y., Yuan, H., Wang, J., Zheng, H., Wang, Y., Cen, X., Xu, F., Bai, J., Han, X., Lu, G., Zhu, Y., Shao, Z., Yan, H., Li, C., Peng, N., Zhang, Z., Zhang, Y., Lin, W., Fan, Y., Qin, Z., Hu, Y., Zhu, B., Wang, S., Ding, X., and Zhao, G. P. (2010) Complete genome sequence of the rifamycin SV-producing *Amycolatopsis mediterranei* U32 revealed its genetic characteristics in phylogeny and metabolism. *Cell. Res.* **20**, 1096-1108
14. Jenkins, V. A., Robertson, B. D., and Williams, K. J. (2012) Aspartate D48 is essential for the GlnR-mediated transcriptional response to nitrogen limitation in *Mycobacterium smegmatis*. *FEMS. Microbiol. Lett.* **330**, 38-45
15. Yu, H., Yao, Y., Liu, Y., Jiao, R., Jiang, W., and Zhao, G. P. (2007) A complex role of *Amycolatopsis mediterranei* GlnR in nitrogen metabolism and related antibiotics production. *Arch. Microbiol.* **188**, 89-96

16. Tiffert, Y., Franz-Wachtel, M., Fladerer, C., Nordheim, A., Reuther, J., Wohlleben, W., and Mast, Y. (2011) Proteomic analysis of the GlnR-mediated response to nitrogen limitation in *Streptomyces coelicolor* M145. *Appl. Microbiol. Biotechnol.* **89**, 1149-1159
17. Wang, Y., Cen, X. F., Zhao, G. P., and Wang, J. (2012) Characterization of a new GlnR binding box in the promoter of amtB in *Streptomyces coelicolor* inferred a PhoP/GlnR competitive binding mechanism for transcriptional regulation of amtB. *J. Bacteriol.* **194**, 5237-5244
18. Wang, J., and Zhao, G. P. (2009) GlnR positively regulates nasA transcription in *Streptomyces coelicolor*. *Biochem Biophys Res Commun* **386**, 77-81
19. Wang, Y., Wang, J. Z., Shao, Z. H., Yuan, H., Lu, Y. H., Jiang, W. H., Zhao, G. P., and Wang, J. (2013) Three of four GlnR binding sites are essential for GlnR-mediated activation of transcription of the *Amycolatopsis mediterranei* nas operon. *J Bacteriol* **195**, 2595-2602
20. Fink, D., Weissschuh, N., Reuther, J., Wohlleben, W., and Engels, A. (2002) Two transcriptional regulators GlnR and GlnRII are involved in regulation of nitrogen metabolism in *Streptomyces coelicolor* A3(2). *Mol. Microbiol.* **46**, 331-347
21. Hutchings, M. I., Hoskisson, P. A., Chandra, G., and Buttner, M. J. (2004) Sensing and responding to diverse extracellular signals? Analysis of the sensor kinases and response regulators of *Streptomyces coelicolor* A3(2). *Microbiology* **150**, 2795-2806
22. Bourret, R. B. (2010) Receiver domain structure and function in response regulator proteins. *Curr. Opin. Microbiol.* **13**, 142-149
23. Hickey, J. M., Lovell, S., Battaile, K. P., Hu, L., Middaugh, C. R., and Hefty, P. S. (2011) The atypical response regulator protein ChxR has structural characteristics and dimer interface interactions that are unique within the OmpR/PhoB subfamily. *J. Biol. Chem.* **286**, 32606-32616
24. O'Connor, T. J., and Nodwell, J. R. (2005) Pivotal roles for the receiver domain in the mechanism of action of the response regulator RamR of *Streptomyces coelicolor*. *J. Mol. Biol.* **351**, 1030-1047.
25. Amon, J., Brau, T., Grimrath, A., Hanssler, E., Hasselt, K., Holler, M., Jessberger, N., Ott, L., Szokol, J., Titgemeyer, F., and Burkovski, A. (2008) Nitrogen control in *Mycobacterium smegmatis*: nitrogen-dependent expression of ammonium transport and assimilation proteins depends on the OmpR-type regulator GlnR. *J. Bacteriol.* **190**, 7108-7116
26. Bertani, G. (2004) Lysogeny at mid-twentieth century: P1, P2, and other experimental systems. *J Bacteriol* **186**, 595-600
27. Mejia, A., Barrios-Gonzalez, J., and Viniegra-Gonzalez, G. (1998) Overproduction of rifamycin B by *Amycolatopsis mediterranei* and its relationship with the toxic effect of barbital on growth. *J. Antibiot. (Tokyo)* **51**, 58-63
28. Kieser, T., and Hopwood, D. A. (1991) Genetic manipulation of Streptomyces: integrating vectors and gene replacement. *Methods. Enzymol.* **204**, 430-458
29. Ma, J., Zhang, P., Zhang, Z., Zha, M., Xu, H., Zhao, G., and Ding, J. (2008) Molecular basis of the substrate specificity and the catalytic mechanism of citramalate synthase from *Leptospira interrogans*. *Biochem. J.* **415**, 45-56
30. Boulanger, A., Chen, Q., Hinton, D. M., and Stibitz, S. (2013) In vivo phosphorylation dynamics of the *Bordetella pertussis* virulence-controlling response regulator BvgA. *Mol. Microbiol.* **88**, 156-172
31. Sheridan, R. C., McCullough,J.F., Wakefield ,Z.T. . (1971) Phosphoramidic acid and its salts. *Inorg. Synth.* **13**, 23-26
32. Kinoshita, E., Kinoshita-Kikuta, E., Takiyama, K., and Koike, T. (2006) Phosphate-binding tag, a new tool to visualize phosphorylated proteins. *Mol. Cell. Proteomics.* **5**, 749-757
33. Barbieri, C. M., and Stock, A. M. (2008) Universally applicable methods for monitoring response regulator aspartate phosphorylation both in vitro and in vivo using Phos-tag-based reagents. *Anal. Biochem.* **376**, 73-82

34. Adams, P. D., Grosse-Kunstleve, R. W., Hung, L. W., Ioerger, T. R., McCoy, A. J., Moriarty, N. W., Read, R. J., Sacchettini, J. C., Sauter, N. K., and Terwilliger, T. C. (2002) PHENIX: building new software for automated crystallographic structure determination. *Acta. Crystallogr. D. Biol. Crystallogr.* **58**, 1948-1954
35. Emsley, P., and Cowtan, K. (2004) Coot: model-building tools for molecular graphics. *Acta. Crystallogr. D. Biol. Crystallogr.* **60**, 2126-2132
36. Hess, B., Kutzner, C., van der Spoel, D., and Lindahl, E. (2008) GROMACS 4: Algorithms for Highly Efficient, Load-Balanced, and Scalable Molecular Simulation. *J. Chem. Theory. Comput.* **4**, 435-447
37. Piana, S., Lindorff-Larsen, K., and Shaw, D. E. (2011) How robust are protein folding simulations with respect to force field parameterization. *Biophys. J.* **100**, 47-49
38. Bussi, G., Donadio, D., and Parrinello, M. (2007) Canonical sampling through velocity rescaling. *J. Chem. Phys.* **126**, 014101
39. Yu, H., Peng, W. T., Liu, Y., Wu, T., Yao, Y. F., Cui, M. X., Jiang, W. H., and Zhao, G. P. (2006) Identification and characterization of glnA promoter and its corresponding trans-regulatory protein GlnR in the rifamycin SV producing actinomycete, *Amycolatopsis mediterranei* U32. *Acta. Biochim. Biophys. Sin. (Shanghai)* **38**, 831-843
40. Ding, X. M., Zhang, N., Tian, Y. Q., Jiang, W. H., Zhao, G. P., and Jiao, R. S. (2002) Establishment of gene replacement/disruption system through homologous recombination in *Amycolatopsis mediterranei* U32. *Sheng Wu Gong Cheng Xue Bao* **18**, 431-437
41. Shu, D., Chen, L., Wang, W., Yu, Z., Ren, C., Zhang, W., Yang, S., Lu, Y., and Jiang, W. (2009) afsQ1-Q2-sigQ is a pleiotropic but conditionally required signal transduction system for both secondary metabolism and morphological development in *Streptomyces coelicolor*. *Appl. Microbiol. Biotechnol.* **81**, 1149-1160
42. McCleary, W. R. (1996) The activation of PhoB by acetylphosphate. *Mol. Microbiol.* **20**, 1155-1163
43. Darbon, E., Martel, C., Nowacka, A., Pegot, S., Moreau, P. L., and Virolle, M. J. (2012) Transcriptional and preliminary functional analysis of the six genes located in divergence of phoR/phoP in *Streptomyces lividans*. *Appl. Microbiol. Biotechnol.* **95**, 1553-1566
44. Wang, L., Tian, X., Wang, J., Yang, H., Fan, K., Xu, G., Yang, K., and Tan, H. (2009) Autoregulation of antibiotic biosynthesis by binding of the end product to an atypical response regulator. *Proc. Natl. Acad. Sci. U S A* **106**, 8617-8622
45. Gao, R., Mukhopadhyay, A., Fang, F., and Lynn, D. G. (2006) Constitutive activation of two-component response regulators: characterization of VirG activation in *Agrobacterium tumefaciens*. *J. Bacteriol.* **188**, 5204-5211
46. Arribas-Bosacoma, R., Kim, S. K., Ferrer-Orta, C., Blanco, A. G., Pereira, P. J., Gomis-Rüth, F. X., Wanner, B. L., Coll, M., and Solà, M. (2007) The X-ray crystal structures of two constitutively active mutants of the *Escherichia coli* PhoB receiver domain give insights into activation. *J. Mol. Biol.* **366**, 626-641
47. Friedland, N., Mack , T. R., Yu, M., Hung, L. W., Terwilliger, T. C., Waldo, G. S., and Stock, A. M. (2007) Domain orientation in the inactive response regulator *Mycobacterium tuberculosis* MtrA provides a barrier to activation. *Biochemistry* **46**, 6733-6743
48. Nowak, E., Panjikar, S., Konarev, P., Svergun, D. I., and Tucker, P. A. (2006) The structural basis of signal transduction for the response regulator PrrA from *Mycobacterium tuberculosis*. *J. Biol. Chem.* **281**, 9659-9666
49. Robinson, V. L., Wu, T., and Stock, A. M. (2003) Structural analysis of the domain interface in DrrB, a response regulator of the OmpR/PhoB subfamily. *J. Bacteriol.* **185**, 4186-4194
50. West, A. H., and Stock, A. M. (2001) Histidine kinases and response regulator proteins in two-component signaling systems. *Trends. Biochem. Sci.* **26**, 369-376

51. Lewis, R. A., Shahi, S. K., Laing, E., Bucca, G., Efthimiou, G., Bushell, M., and Smith, C. P. (2011) Genome-wide transcriptomic analysis of the response to nitrogen limitation in *Streptomyces coelicolor* A3(2). *BMC. Res. Notes.* **4**, 78
52. Appleby, J. L., and Bourret, R. B. (1999) Activation of CheY mutant D57N by phosphorylation at an alternative site, Ser-56. *Mol. Microbiol.* **34**, 915-925.
53. Thao, S., Chen, C. S., Zhu, H., and Escalante-Semerena, J. C. (2010) Nepsilon-lysine acetylation of a bacterial transcription factor inhibits Its DNA-binding activity. *PLoS. One.* **5**, e15123
54. Hu, L. I., Chi, B. K., Kuhn, M. L., Filippova, E. V., Walker-Peddakotla, A. J., Basell, K., Becher, D., Anderson, W. F., Antelmann, H., and Wolfe, A. J. (2013) Acetylation of the Response Regulator RcsB Controls Transcription from a Small RNA Promoter. *J. Bacteriol.* **195**, 4174-4186
55. Zakikhany, K., Harrington, C. R., Nimtz, M., Hinton, J. C., and Römling, U. (2010) Unphosphorylated CsgD controls biofilm formation in *Salmonella enterica* serovar Typhimurium. *Mol Microbiol* **77**, 771-786

Acknowledgements-We thank the staffs at the Shanghai synchrotron facility beamline 17U1 for their technical assistance in data collection. This work is supported by grants from the National Basic Research Program of China (2012CB721102), National Nature Science Foundation (31322016, 31121001 and 30830002) and the Shanghai Institutes for Biological Sciences, Chinese Academy of Sciences (2012OHTP, 2009CSP001, and KSCX2-EW-J-12). The structures of AmeGlnRRec and MtbGlnRRec have been deposited in the Protein Data Bank with the accession code 4O1H and 4O1I.

FIGURE LEGENDS

Figure 1. Biochemical analyses detecting the phosphorylation status of the conserved residue Asp of GlnR. A. Western blot monitoring the phosphorylation status of the His-tag fused *E. coli* PhoB (EcoPhoB), *S. coelicolor* GlnR/5403 (ScoGlnR/SCO5403), *A. mediterranei* U32 GlnR (AmeGlnR) and the *A. mediterranei* U32 PhoP (AmePhoP), purified by Ni-affinity chromatography from the corresponding *E. coli* heterologous expression systems (*Materials* and *Methods*) treated with (+) or without (-) 20 mM ammonium hydrogen phosphoramidate (PA). **B.** Western blot monitoring the *in vivo* phosphorylation status of the Flag-tag fused PhoP (WT, D52A) under the phosphate replete (K_2HPO_4) or limited (-) conditions, and the phosphorylation status of Flag-tag fused GlnR(WT, D50A) under nitrogen rich ($(NH_4)_2SO_4$) or limited (KNO_3) conditions in the *A. mediterranei* U32Δ*glnR* and *S.coelicolor* M145Δ*glnR* strains, cell lysates were treated as described in *Materials* and *Methods* .

Figure 2. Structure and comparison of different GlnRRecs. A. Structural-based sequence alignment of different GlnRRecs. The 5 residues constituting the phosphorylation pocket in typical RRs are highlighted in red, while the corresponding residues differ from typical RRs in GlnR and atypical RRs are shown in yellow. The highly conserved residues among OmpR subfamily RRs are colored in blue, and the residues only shown conservation among GlnRs are colored in cyan. Red stars indicate the conformation switch residues in typical RRs; Red triangle indicates the conserved residue Asp in the putative phosphorylation site; Red circles indicate the two residues Thr and Arg forming interactions with the residue Asp in the putative phosphorylation site; Red square indicates the Arg residue essential for the dimerization. The secondary structure elements of AmeGlnR and PhoB (PDB ID, 1ZES) are shown at top and bottom, respectively. AmeGlnR, GlnR from *A. mediterranei* U32 (YP_003771100); MtbGlnR, GlnR from from *M. tuberculosis* H37Rv (NP_215333); ScoGlnR, GlnR from *S. coelicolor* M145 (NP_628336); MseGlnR, GlnR from *M. smegmatis strain* MC2 155 (YP_890012); SveGlnR, GlnR from *S. venezuelae* ATCC 10712 (YP006879462). ChxR is from *C. trachomatis* 434/Bu (YP_001654963); NblR is from *Synechococcus elongatus* PCC 7942(AAC33849); HP1043 is from *H. pylori* (NP_207833); JadR1 is from *S. venezuelae* ATCC 10712(AAB36584); ArcA is from *E. coli* K12 (NP_418818); OmpR is from *E. coli* O157:H7 strain EDL933 (NP_289945); PhoB is from *E. coli* K12 (NP_414933). **B.** Ribbon diagram shows the structure of the AmeGlnRRec. The two molecules A and B constituting the homodimer are colored in yellow and cyan, the dimer interface is shown in magenta. **C.** Structure comparison of AmeGlnRRec (cyan) with phosphorylated PhoB (grey) (PDB ID 1ZES). β1-α1 and β3-α3 loops and residue Arg52 of AmeGlnRRec are colored in magenta. The residues important for phosphorylation in PhoB and corresponding ones in AmeGlnRRec are shown with side chains. A close-up view of the putative phosphorylation pocket and interactions are also shown.

Figure 3. Structure and *in vitro* characterization of the residues essential for AmeGlnRRec homodimer interaction. A. Sequence alignment of the residues constituting the dimer interface of GlnR, ChxR, HP1043, ArcA, PhoB, the hydrophobic and hydrophilic residues are colored in yellow and green, respectively. **B.** Superimposition of the structural elements involved in the homodimer interface of AmeGlnRRec (magenta) and PhoB (grey). **C.** Residues involved in the homodimer formation. The two molecules are colored in yellow and cyan. Hydrophobic interaction residues are shown with spheres, hydrophilic residues forming hydrogen bonds and salt bridges (shown with red dashed lines and numbers indicating the distance) are shown with side chains. **D.** Gel filtration analysis of wild-type AmeGlnRRec and its mutants. The mobility profiles of wild-type AmeGlnRRec, R111A, D50A, D50N and D50E are shown, the molecular masses are calculated based on the standard proteins indicated on the top. The 25, 40 kDa peaks represent the monomer and dimer respectively, while the 64,70kDa peak represents the oligomer.

Figure 4. *In vivo* cross-linking analysis of AmeGlnR and its mutants. The oligomeric status of the wild type and mutated AmeGlnR (R111A, D50A, D50N, T9A, R52A and T9A/R52A, D50E) in the presence (+) and absence (-) of cross-linking agent DSS are shown by western blot analysis. The strains were cultured in the nitrogen-rich ($(NH_4)_2SO_4$) or limited (KNO_3) conditions. Molecular markers are shown on the left. Di, dimer; Mo, monomer.

Figure 5. Growth phenotypes of *A. mediterranei* U32 mutants and complementation strains. Results of complementation by wild-type *AmeglnR* or the *glnR* mutants (R111A/E, D50A, D50N, D50E, T9A, R52A and T9A/R52A) grown on minimal medium supplemented with KNO_3.

Figure 6. Transcriptional analysis of wild type U32 and *glnR* mutants for the transcription of GlnR target genes in *A.mediterranei* . The transcription of *rpoB* was used as the internal control. Abbreviations: WT, wild-type *A.mediterranei* U32; Δ, U32Δ*glnR*; +, *AmeglnR*+; D50A, *AmeglnR*(D50A); D50E, *AmeglnR*(D50E); D50N, *AmeglnR*(D50N); T9A, *AmeglnR*(T9A); R52A, *AmeglnR*(R52A);T9A/R52A,*AmeglnR*(T9A/R52A);R111A,*AmeglnR*(R111A);R111E,*AmeglnR*(R111E); Am, Bennet medium with 60mM ammonium; Ni, Bennet medium with 80mM KNO3.

Figure 7. EMSA results of wild type AmeGlnR and its mutants. The FAM-labeled *glnA* promoter region was incubated with the indicated concentrations of AmeGlnR proteins (WT, D50A, D50E, D50N, T9A, R52A, T9A/R52A, R111A and R111E), and salmon sperm DNA was added in each sample to mask the non-specific binding effect. The signal of free DNA and protein-DNA complexes were scanned and shown.

Figure 8. Structural differences between wild type AmeGlnRRec dimer and AmeGlnRRec (D50A, MD simulations). The structure of wild type AmeGlnRRec dimer is colored gray, the MD simulated structure of AmeGlnRRec (D50A) is colored yellow (molecule A) and cyan (molecule B). The β3-α3 loop (residues Ala50-Asp54) and β4-α4 loop (residues Val81-Val86) are colored in magenta, arrow indicates the significant conformational change in β4-α4 loop. The residues constituting the putative phosphorylation pocket and the polar residues involved in the dimer interface are shown with sticks.

Figure 9. Different conformations of the "switch residues" in AmeGlnRRec and PhoB. A. The conformations of the "switch residues" in AmeGlnRRec (Val81 and Ile98, shown with blue sticks) differ from those in phosphorylated PhoB (green stick); **B.** but are similar to those in unphosphorylated PhoB (yellow stick). The PDB IDs of phosphorylated and unphosphorylated PhoB are 1ZES and 1B00, respectively.

Table 1. Statistics of diffraction data collection and structure refinement

	MtbGlnRRec	AmeGlnRRec	AmeGlnRRec-Se
Diffraction data			
Wavelength (Å)	0.9793	0.9793	0.9793
Space group	I41	$P6_522$	$P6_522$
Cell parameters			
a (Å)	144.2	93.1	93.1
b (Å)	144.2	93.1	93.1
c (Å)	92.2	308.4	310.4
α (°)	90.0	90.0	90
β (°)	90.0	90.0	90
γ (°)	90.0	120.0	120
Resolution (Å)	50.0-2.80 (2.90-2.80)[a]	50.0-2.80 (2.90-2.80)	50.0-3.00 (3.11-3.00)
Observed reflections	71,225	196,781	698891
Unique reflections (I/σ(I) > 0)	23,093	20,511	16902
Average redundancy	3.1 (3.1)	9.6 (9.9)	41.3 (42.8)
Average I/σ(I)	13.7 (4.4)	19.1 (4.4)	54.8 (10.9)
Completeness (%)	99.0 (99.7)	99.8 (100.0)	100.0 (100.0)
R_{merge} (%)[b]	9.8 (31.9)	11.7 (62.1)	16.0 (63.0)
Refinement and structure model			
Reflections ($Fo \geq 0\sigma(Fo)$)			
Working set	21,918	19,390	
Test set	1,158	1,039	
R_{work}/R_{Free} (%)[c]	18.0 / 22.5	22.1 / 26.9	
No. of atoms	4,283	3,391	
Protein	4,111	3,364	
Water	172	27	
Average B factor (Å^2)			
All atoms	38.8	54.5	
Protein	38.8	54.6	
Water	38.5	50.3	
RMS deviations			
Bond lengths (Å)	0.007	0.011	
Bond angles (°)	1.4	1.9	
Ramachandran plot (%)			
Most favoured	95.3	97.6	
Allowed	4.7	2.4	

[a] Numbers in parentheses represent the highest resolution shell.

[b] $Rmerge=\sum_{hkl}\sum_i|I_i(hkl)-<I(hkl)>|/\sum_{hkl}\sum_i I_i(hkl)$.

[c] $R=\sum_{hkl}||F_o|-|F_c||/\sum_{hkl}|F_o|$.

Figure 1

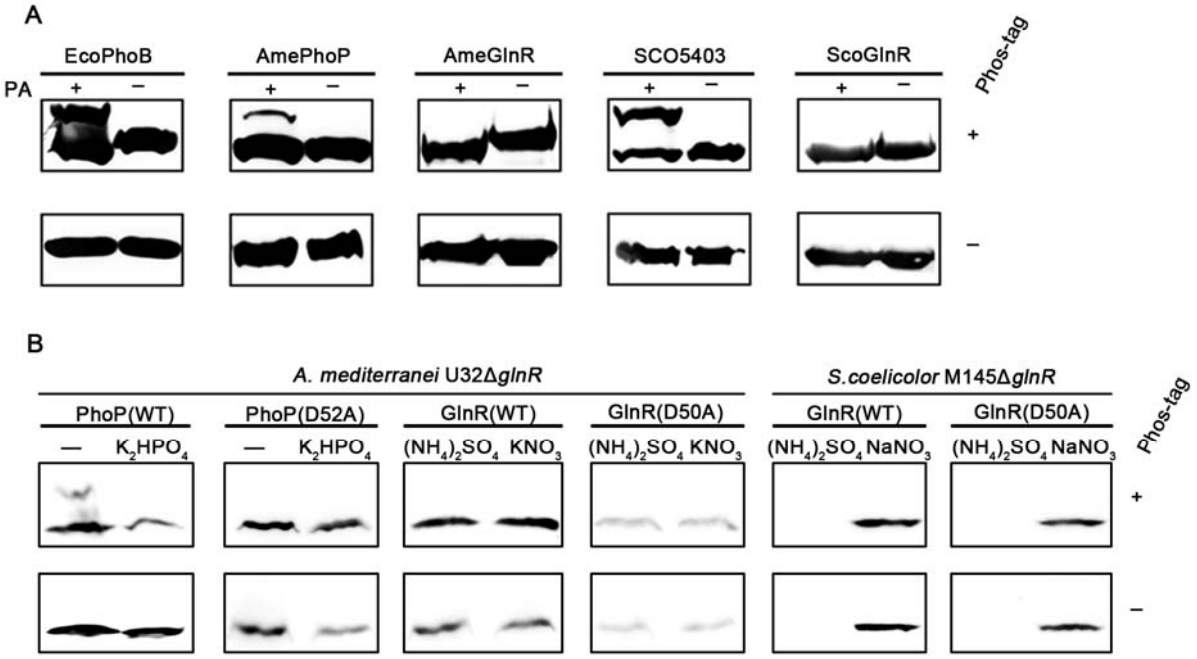

Figure 2

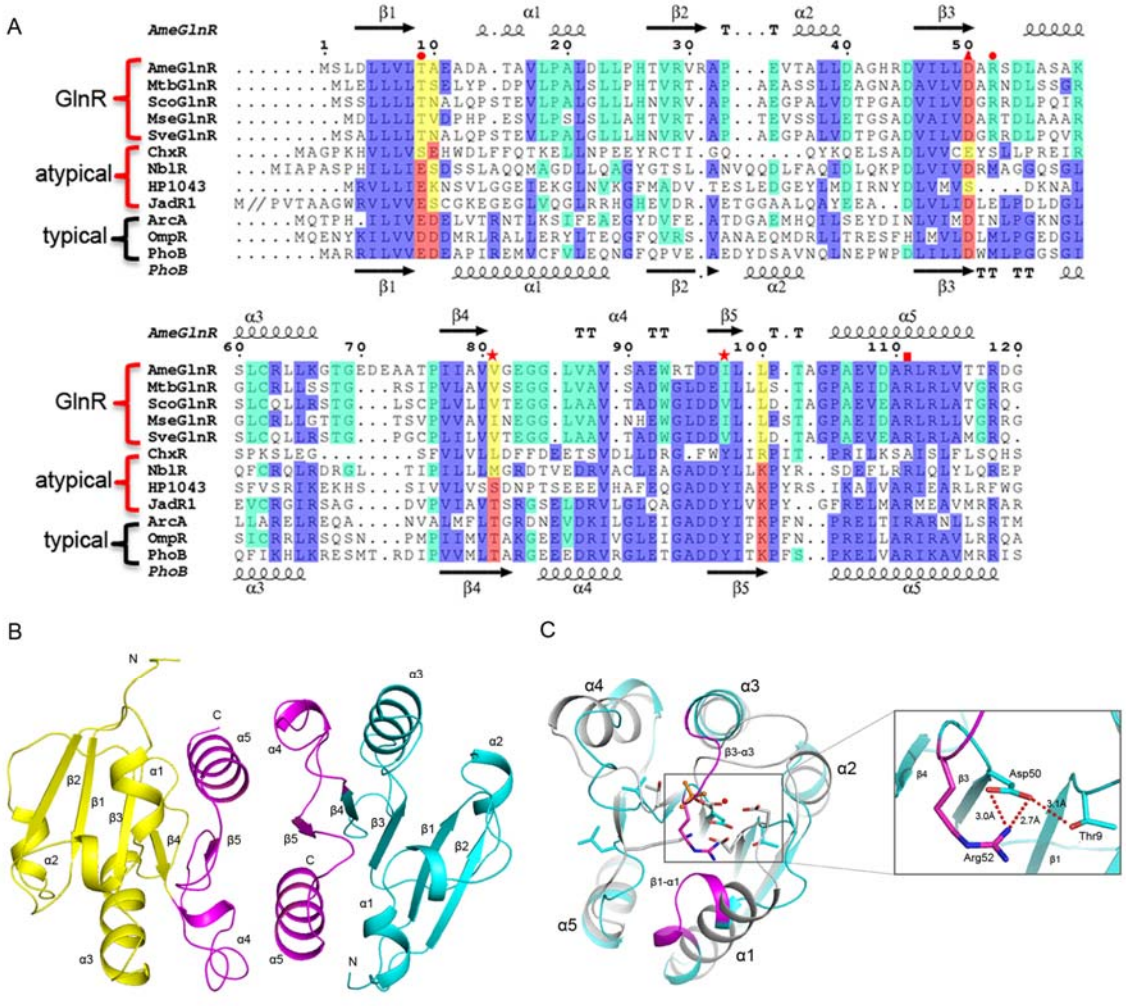

Figure 3

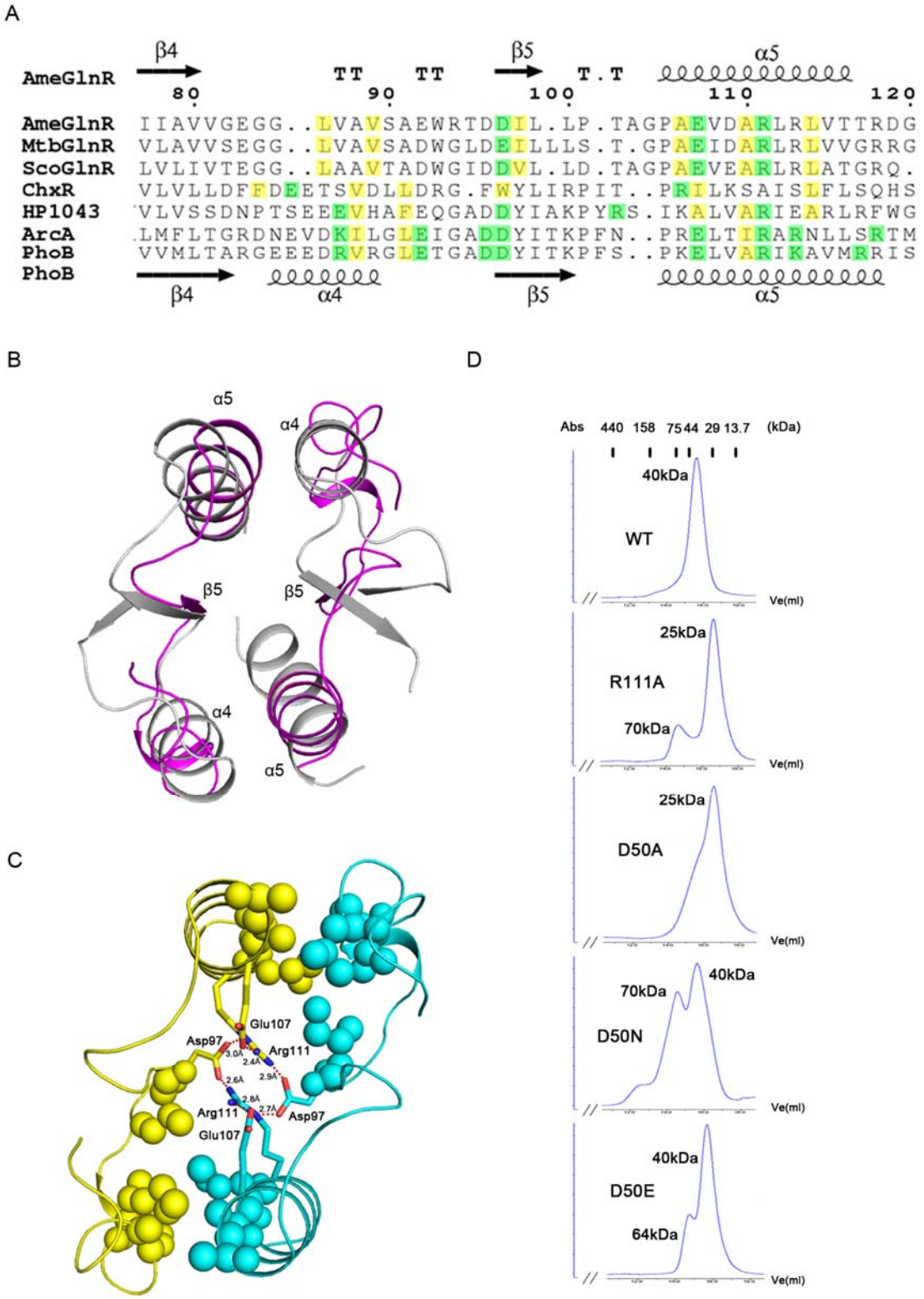

Figure 4

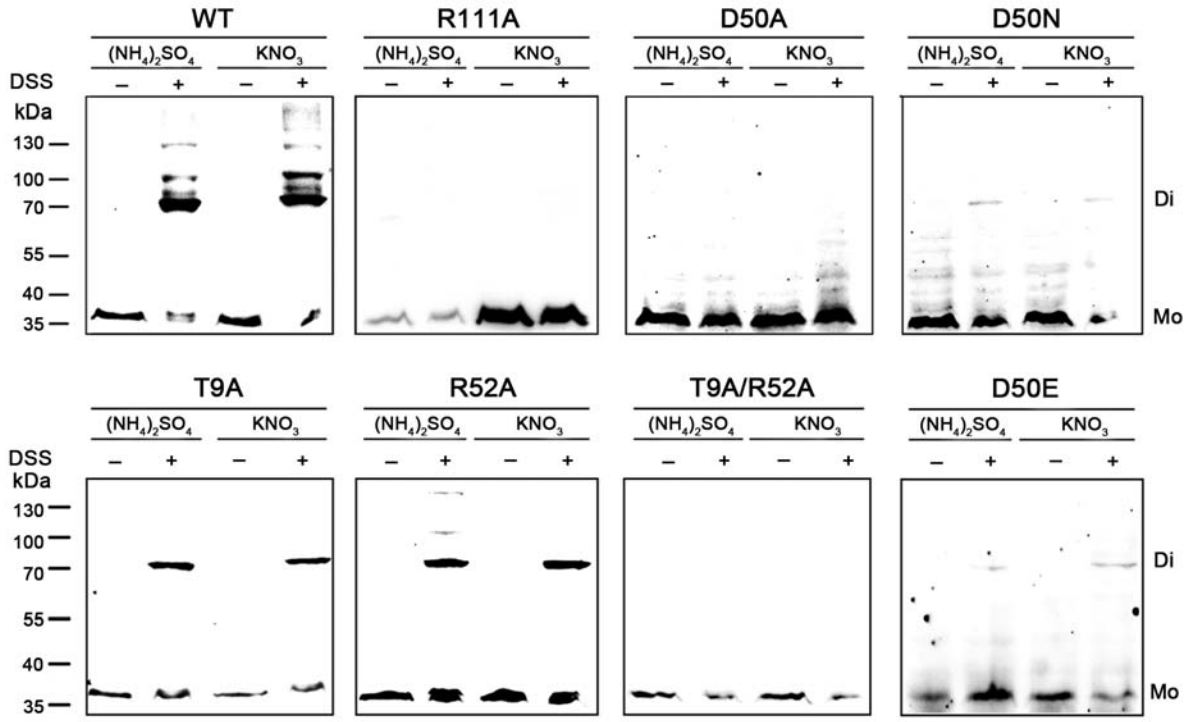

Figure 5

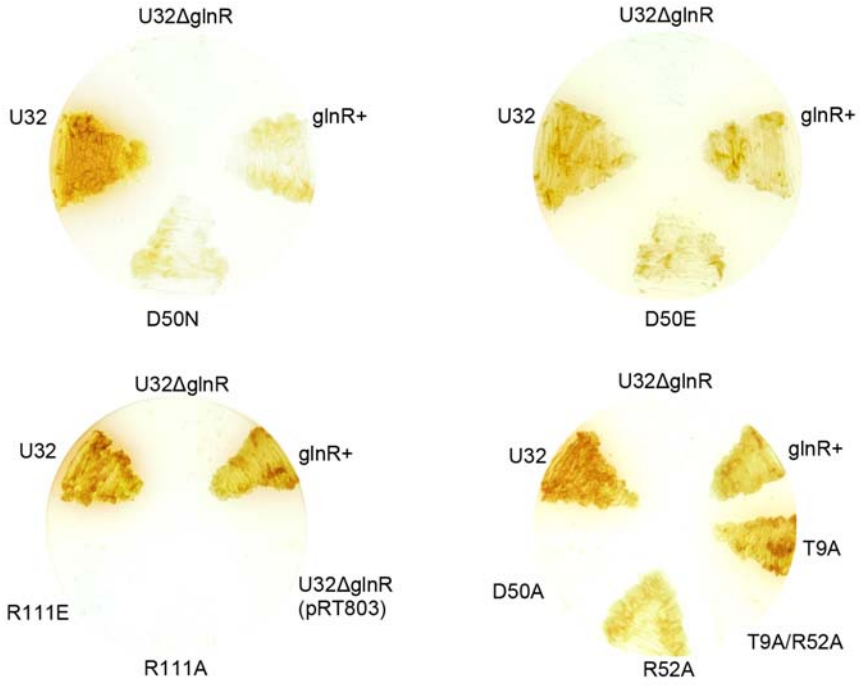

Figure 6

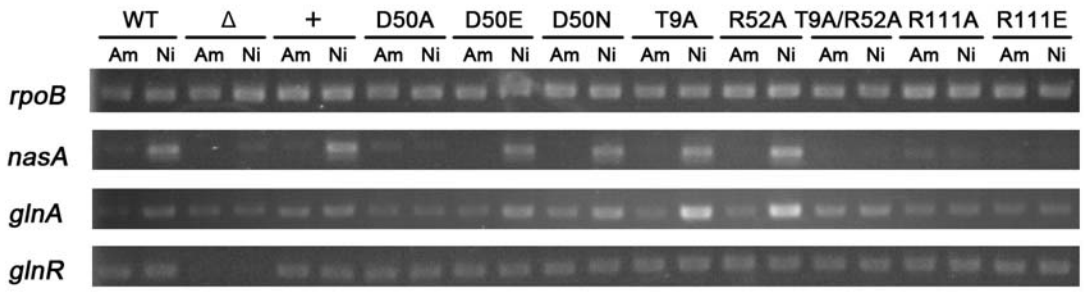

Figure 7

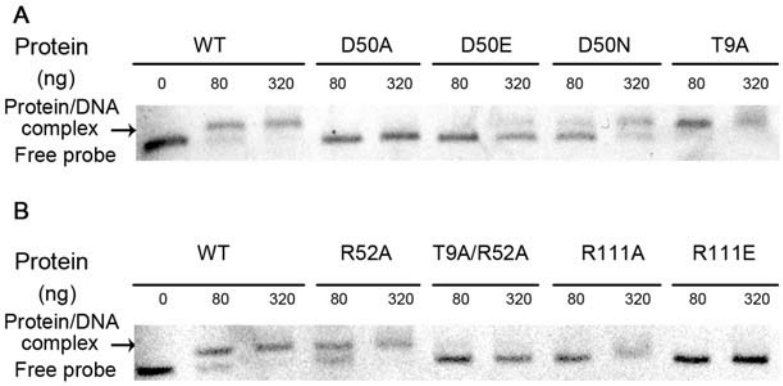

Figure 8

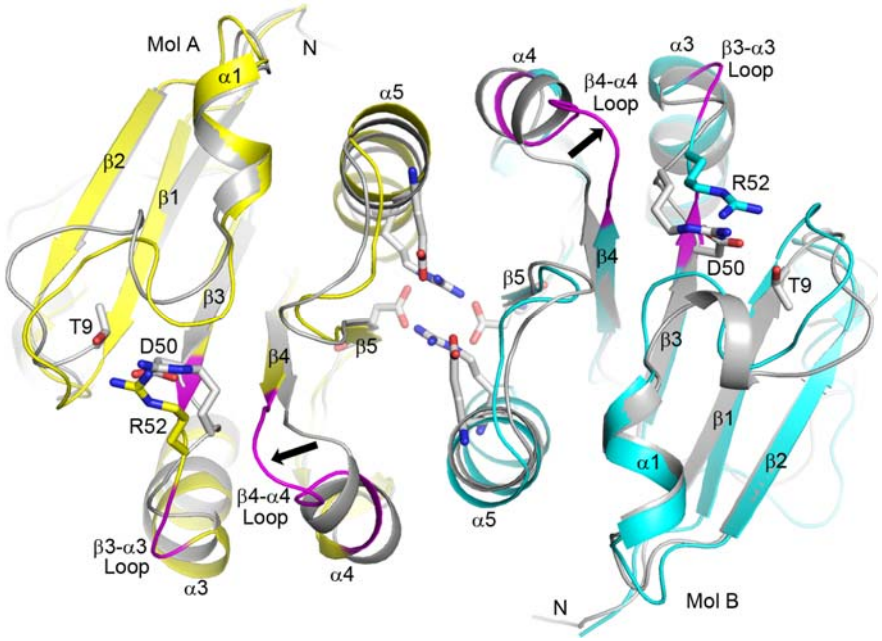

Figure 9

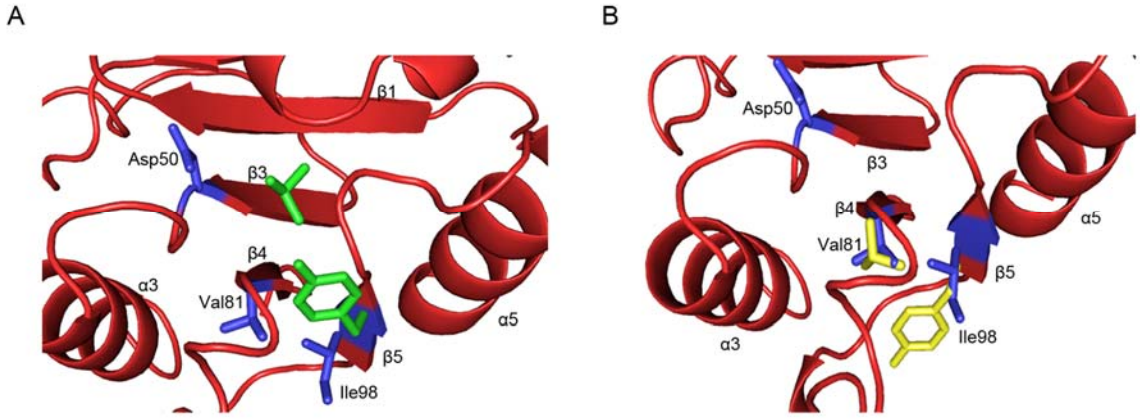

Atypical OmpR/PhoB Subfamily Response Regulator GlnR of Actinomycetes Functions as a Homodimer, Stabilized by the Unphosphorylated Conserved Asp-focused Charge Interactions

Wei Lin, Ying Wang, Xiaobiao Han, Zilong Zhang, Chengyuan Wang, Jin Wang, Huaiyu Yang, Yinhua Lu, Weihong Jiang, Guo-Ping Zhao and Peng Zhang

J. Biol. Chem. published online April 14, 2014
